Inorg. Chem. **2004**, *43*, 3724–3732

Electronic Spectroscopy, Photophysical Properties, and Emission Quenching Studies of an Oxidatively Robust Perfluorinated Platinum Porphyrin

Siu-Wai Lai,[†] Yuan-Jun Hou,[†] Chi-Ming Che,*[,†] Hei-Leung Pang,[‡] Kwok-Yin Wong,[‡] Chi K. Chang,[§] and Nianyong Zhu[†]

Department of Chemistry and Open Laboratory of Chemical Biology of the Institute of Molecular Technology for Drug Discovery and Synthesis, The University of Hong Kong, Pokfulam Road, Hong Kong SAR, China, Department of Applied Biology and Chemical Technology, The Hong Kong Polytechnic University, Hunghom, Kowloon, Hong Kong SAR, China, and Department of Chemistry, Hong Kong University of Science and Technology, Clear Water Bay, Kowloon, Hong Kong SAR, China

Received January 25, 2004

The highly electron-deficient, β-octafluorinated *meso*-tetrakis(pentafluorophenyl)-porphyrin ($H_2F_{28}TPP$) was metalated with platinum to afford the oxidatively robust luminophore [$PtF_{28}TPP$], and its X-ray structure shows that the porphyrin core exists in a slightly saddle-shaped conformation. The absorption spectrum of [$PtF_{28}TPP$] in CH_2Cl_2 displays a near-UV Soret band (B) at 383 nm ($\epsilon = 2.85 \times 10^5$ dm^3 mol^{-1} cm^{-1}) and two visible Q(1,0) and Q(0,0) bands at 501 ($\epsilon = 1.45 \times 10^4$ dm^3 mol^{-1} cm^{-1}) and 533 ($\epsilon = 1.36 \times 10^4$ dm^3 mol^{-1} cm^{-1}) nm, respectively. These absorption bands of [$PtF_{28}TPP$] are blue-shifted from those in [$PtF_{20}TPP$] (390, 504, and 538 nm, respectively) and [PtTPP] (401, 509, and 539 nm, respectively). Excitation of [$PtF_{28}TPP$] (complex concentration $= 1.5 \times 10^{-6}$ mol dm^{-3}) in dichloromethane at the Soret or Q(1,0) or Q(0,0) band gave a phosphorescence with peak maximum at 650 nm (lifetime = 5.8 μs) and a weak shoulder at 712 nm. Both the emission lifetime and quantum yield vary with solvent polarity, and plots of τ versus E_K and Φ versus E_K (where E_K is the empirical solvent polarity parameter based on the hypsochromic shift of the longest wavelength absorption of the [$Mo(CO)_4\{(C_5H_4N)HC{=}NCH_2C_6H_5\}$] complex with increasing solvent polarity; see: Kamlet, M. J.; Abboud, J. L. M.; Taft, R. W. *Prog. Phys. Org. Chem.* **1981**, *13*, pp 485–630) show linear correlation, indicating that the emission is sensitive to the local environment/medium. Electrochemical studies on [$PtF_{28}TPP$] by cyclic voltammetry showed no porphyrin-centered oxidation at potential $\leq$ 1.5 V versus Ag/$AgNO_3$, demonstrating that [$PtF_{28}TPP$] is more resistant toward oxidation than [PtF_{20}-TPP] ($E_{1/2} = 1.33$ V) and [PtTPP] ($E_{1/2} = 0.97$ V). The porphyrin-centered reduction of [$PtF_{28}TPP$] occurs at –0.75 and –1.18 V, which is anodically shifted from those at –1.06 and –1.55 V in [$PtF_{20}TPP$], and –1.51 V in [PtTPP], respectively. The excited-state reduction potential of [$PtF_{28}TPP$] is estimated to be 1.49 V versus Ag/$AgNO_3$. Over 97% of the emission intensity of [$PtF_{28}TPP$] was retained after irradiation with a high power mercury arc lamp (500 W) for 14 h, compared to 90% and 12% for [$PtF_{20}TPP$] and [PtTPP], respectively; hence, [$PtF_{28}TPP$] exhibits superior photostability. Quenching of the emission of [$PtF_{28}TPP$] by oxygen, alcohol, catechol, and butylamine reveals that [$PtF_{28}TPP$] is an oxidatively robust material with medium-sensitive photoluminescence properties.

Introduction

Halogenated metalloporphyrins are well documented to be robust toward oxidative degradation. The reactivities and properties of this class of compounds can be modulated by electron-withdrawing substituents at the *meso*-aryl[1] and/or β-pyrrolic[2] positions; for example, the redox potentials of metalloporphyrins[3] are anodically shifted upon incorporation

* To whom correspondence should be addressed. E-mail: cmche@hku.hk.
[†] The University of Hong Kong.
[‡] The Hong Kong Polytechnic University.
[§] Hong Kong University of Science and Technology.

(1) (a) Chang, C. K.; Ebina, F. *J. Chem. Soc., Chem. Commun.* **1981**, 778−779. (b) Traylor, P. S.; Dolphin, D.; Traylor, T. G. *J. Chem. Soc., Chem. Commun.* **1984**, 279−280. (c) Dicken, C. M.; Woon, T. C.; Bruice, T. C. *J. Am. Chem. Soc.* **1986**, *108*, 1636−1643. (d) Ellis, P. E., Jr.; Lyons, J. E. *J. Chem. Soc., Chem. Commun.* **1989**, 1315−1316.

10.1021/ic049902h CCC: $27.50
Published on Web 05/15/2004

of halogen substituents. Previous studies showed that direct substitution at the pyrrolic positions with electron-withdrawing groups has a more pronounced effect on the electrochemical properties of porphyrin rings than derivatization at the *meso*-aryl periphery.[2b,4] β-Pyrrolic substitution also imparts significant perturbation upon the electronic properties of the porphyrin ring, which subsequently affects the HOMO (highest occupied molecular orbital) and LUMO (lowest occupied molecular orbital) levels of the corresponding metalloporphyrins.[5] The increase in redox potentials for metalloporphyrins bearing halogenated substituents can lead to significant changes in the spectroscopic and photochemical properties, including improved stability toward oxidative decomposition which can be useful for application studies in materials science.[6,7]

The perfluorinated 2,3,7,8,12,13,17,18-octafluoro-5,10,15,20-tetrakis(pentafluorophenyl)porphyrin ($H_2F_{28}TPP$) is of particular interest in the context of its exceptional stability toward oxidative degradation and the substantial anodic shift in oxidation potential for the porphyrinato ring.[8] Previous works on halogenated metalloporphyrins have mainly focused on structural, electronic and electrochemical properties, and catalytic activities.[9−11] Structural deviation from planarity in the saddle-shaped molecular structures of chloro- and bromo-substituted metalloporphyrins is known to induce red shifts of the porphyrin absorptions[12] due to a decrease in the HOMO−LUMO energy gap, whereas incorporation of strongly electron-withdrawing fluorine substituents can destabilize the HOMOs effectively to afford blue-shifted absorptions.[13,14]

We now describe the structure and photophysical and electrochemical properties of the [β-octafluoro-*meso*-tetrakis(pentafluorophenyl)porphyrinato]platinum(II) complex [PtF_{28}TPP], and comparisons with [*meso*-tetrakis(pentafluorophenyl)porphyrinato]platinum(II) [$PtF_{20}TPP$][15] and the nonfluorinated congener [PtTPP] (H_2TPP = 5,10,15,20-tetraphenylporphyrin) are presented. The [$PtF_{28}TPP$] complex is demonstrated to be an extremely oxidatively robust phosphorescent material with medium-sensitive emission properties.

Experimental Section

Synthesis and General Procedures. $H_2F_{28}TPP$[8] and [$PtCl_2(NCPh)_2$][16] were prepared by literature methods. [$PtF_{28}TPP$] was synthesized by a procedure similar to that for [$PtF_{20}TPP$].[15] $H_2F_{28}TPP$ (0.50 g, 0.45 mmol) and [$PtCl_2(NCPh)_2$] (0.26 g, 0.55 mmol) were suspended in anhydrous degassed benzonitrile (100 mL). The mixture was heated at 190 °C under a nitrogen atmosphere for 12 h, and then cooled to room temperature. The solvent was removed by vacuum distillation, and the crude product was purified by column chromatography using CH_2Cl_2 as eluent (0.48 g, 81% yield). ^{19}F NMR (400 MHz, $CDCl_3$): δ −138.31 (8F, m, *ortho*-C_6F_5), −145.03 (8F, s, β-F), −149.65 (4F, t, $^3J_{F-F}$ = 20.6 Hz, *para*-C_6F_5), −161.10 (8F, m, *meta*-C_6F_5). FAB-MS: *m*/*z* 1311 [M^+], 1293 [M^+ − F], 1275 [M^+ − 2F]. Anal. Calcd for $C_{44}F_{28}N_4Pt$: C, 40.29; N, 4.27. Found: C, 40.35; N, 4.73.

Fast atom bombardment (FAB) mass spectra were obtained on a Finnigan Mat 95 mass spectrometer. ^{19}F (376 MHz) NMR spectra were recorded on a Bruker Avance 400 FT-NMR spectrometer with chemical shift (in ppm) relative to trifluoroacetic acid. Elemental analyses were performed by the Institute of Chemistry at the Chinese Academy of Sciences, Beijing. Cyclic voltammetry was performed using a Bioanalytical Systems (BAS) model 100 B/W electrochemical analyzer. The electrochemical cell was a conventional two-compartment cell with a glassy carbon disk as the working electrode, a $Ag|AgNO_3$ (0.1 M) electrode as the reference electrode, and a platinum wire as the counter electrode. Tetrabutylammonium hexafluorophosphate (0.1 M) was used as the supporting electrolyte. The ferrocenium/ferrocene was used as internal reference and was observed at 0.19 V versus the $Ag/AgNO_3$ electrode. The $E_{1/2}$ values were taken as the average of the cathodic and anionic peak potentials for the oxidative and reductive waves.

(2) (a) Traylor, T. G.; Tsuchiya, S. *Inorg. Chem.* **1987**, *26*, 1338−1339. (b) Wijesekera, T.; Matsumoto, A.; Dolphin, D.; Lexa, D. *Angew. Chem., Int. Ed. Engl.* **1990**, *29*, 1028−1030. (c) Lyons, J. E.; Ellis, P. E., Jr.; Myers, H. K., Jr. *J. Catal.* **1995**, *155*, 59−73. (d) Ozette, K.; Leduc, P.; Palacio, M.; Bartoli, J.-F.; Barkigia, K. M.; Fajer, J.; Battioni, P.; Mansuy, D. *J. Am. Chem. Soc.* **1997**, *119*, 6442−6443.

(3) (a) Giraudeau, A.; Callot, H. J.; Gross, M. *Inorg. Chem.* **1979**, *18*, 201−206. (b) Giraudeau, A.; Louati, A.; Callot, H. J.; Gross, M. *Inorg. Chem.* **1981**, *20*, 769−772. (c) Bhyrappa, P.; Krishnan, V. *Inorg. Chem.* **1991**, *30*, 239−245.

(4) (a) Callot, H. J.; Giraudeau, A.; Gross, M. *J. Chem. Soc., Perkin Trans. 2* **1975**, 1321−1324. (b) Giraudeau, A.; Callot, H. J.; Jordan, J.; Ezhar, I.; Gross, M. *J. Am. Chem. Soc.* **1979**, *101*, 3857−3862. (c) Giraudeau, A.; Louati, A.; Gross, M.; Callot, H. J.; Hanson, L. K.; Rhodes, R. K.; Kadish, K. M. *Inorg. Chem.* **1982**, *21*, 1581−1586.

(5) Binstead, R. A.; Crossley, M. J.; Hush, N. S. *Inorg. Chem.* **1991**, *30*, 1259−1264.

(6) (a) Wagner, R. W.; Lindsey, J. S.; Seth, J.; Palaniappan, V.; Bocian, D. F. *J. Am. Chem. Soc.* **1996**, *118*, 3996−3997. (b) Li, F.; Gentemann, S.; Kalsbeck, W. A.; Seth, J.; Lindsey, J. S.; Holten, D.; Bocian, D. F. *J. Mater. Chem.* **1997**, *7*, 1245−1262. (c) Strachan, J.-P.; Gentemann, S.; Seth, J.; Kalsbeck, W. A.; Lindsey, J. S.; Holten, D.; Bocian, D. F. *Inorg. Chem.* **1998**, *37*, 1191−1201.

(7) (a) Baldo, M. A.; O'Brien, D. F.; You, Y.; Shoustikov, A.; Sibley, S.; Thompson, M. E.; Forrest, S. R. *Nature* **1998**, *395*, 151−154. (b) O'Brien, D. F.; Baldo, M. A.; Thompson, M. E.; Forrest, S. R. *Appl. Phys. Lett.* **1999**, *74*, 442−444. (c) Yang, S. I.; Seth, J.; Strachan, J.-P.; Gentemann, S.; Kim, D.; Holten, D.; Lindsey, J. S.; Bocian, D. F. *J. Porphyrins Phthalocyanines* **1999**, *3*, 117−147. (d) Xiang, H.-F.; Yu, S.-C.; Che, C.-M.; Lai, P. T. *Appl. Phys. Lett.* **2003**, *83*, 1518−1520.

(8) (a) Gassman, P. G.; Ghosh, A.; Almlöf, J. *J. Am. Chem. Soc.* **1992**, *114*, 9990−10000. (b) Woller, E. K.; DiMagno, S. G. *J. Org. Chem.* **1997**, *62*, 1588−1593. (c) Smirnov, V. V.; Woller, E. K.; DiMagno, S. G. *Inorg. Chem.* **1998**, *37*, 4971−4978. (d) Nelson, A. P.; DiMagno, S. G. *J. Am. Chem. Soc.* **2000**, *122*, 8569−8570. (e) Smirnov, V. V.; Woller, E. K.; Tatman, D.; DiMagno, S. G. *Inorg. Chem.* **2001**, *40*, 2614−2619.

(9) (a) Mandon, D.; Ochsenbein, P.; Fischer, J.; Weiss, R.; Jayaraj, K.; Austin, R. N.; Gold, A.; White, P. S.; Brigaud, O.; Battioni, P.; Mansuy, D. *Inorg. Chem.* **1992**, *31*, 2044−2049. (b) Birnbaum, E. R.; Hodge, J. A.; Grinstaff, M. W.; Schaefer, W. P.; Henling, L.; Labinger, J. A.; Bercaw, J. E.; Gray, H. B. *Inorg. Chem.* **1995**, *34*, 3625−3632.

(10) Birnbaum, E. R.; Schaefer, W. P.; Labinger, J. A.; Bercaw, J. E.; Gray, H. B. *Inorg. Chem.* **1995**, *34*, 1751−1755.

(11) (a) Hodge, J. A.; Hill, M. G.; Gray, H. B. *Inorg. Chem.* **1995**, *34*, 809−812. (b) Grinstaff, M. W.; Hill, M. G.; Birnbaum, E. R.; Schaefer, W. P.; Labinger, J. A.; Gray, H. B. *Inorg. Chem.* **1995**, *34*, 4896−4902.

(12) (a) Reddy, D.; Ravikanth, M.; Chandrashekar, T. K. *J. Chem. Soc., Dalton Trans.* **1993**, 3575−3580. (b) Takeuchi, T.; Gray, H. B.; Goddard, W. A., III. *J. Am. Chem. Soc.* **1994**, *116*, 9730−9732. (c) Ochsenbein, P.; Ayougou, K.; Mandon, D.; Fischer, J.; Weiss, R.; Austin, R. N.; Jayaraj, K.; Gold, A.; Terner, J.; Fajer, J. *Angew. Chem., Int. Ed. Engl.* **1994**, *33*, 348−350.

(13) Ghosh, A. *J. Am. Chem. Soc.* **1995**, *117*, 4691−4699.

(14) (a) Spellane, P. J.; Gouterman, M.; Antipas, A.; Kim, S.; Liu, Y. C. *Inorg. Chem.* **1980**, *19*, 386-391. (b) DiMagno, S. G.; Wertsching, A. K.; Ross, C. R., II. *J. Am. Chem. Soc.* **1995**, *117*, 8279−8280. (c) Leroy, J.; Bondon, A.; Toupet, L.; Rolando, C. *Chem. Eur. J.* **1997**, *3*, 1890−1893.

(15) Che, C.-M.; Hou, Y.-J.; Chan, M. C. W.; Guo, J.; Liu, Y.; Wang, Y. *J. Mater. Chem.* **2003**, *13*, 1362−1366.

(16) Anderson, G. K.; Lin, M. *Inorg. Synth.* **1990**, *28*, 60−63.

Photophysical Measurements. Absorption spectra were recorded on a Hewlett-Packard HP8453 spectrophotometer. Luminescence spectra were collected by a Spex Fluorolog-double spectrophotometer with a Xe arc lamp excitation source and a Hamamatsu R928P photomultiplier tube. Solution samples for measurements were degassed with at least four freeze−pump−thaw cycles. Luminescence quantum yield of [PtF_{28}TPP] was referenced to [ZnTPP] in benzene ($\Phi = 0.033$) and calculated according to the following equation:[17]

$$\Phi_{unk} = \Phi_{std}\left(\frac{I_{unk}}{A_{unk}}\right)\left(\frac{A_{std}}{I_{std}}\right)\left(\frac{n_{unk}}{n_{std}}\right)^2$$

where Φ_{unk} is the radiative quantum yield of the sample, Φ_{std} is the radiative quantum yield of the standard, I_{unk} and I_{std} are the integrated emission intensities of the sample and standard, A_{unk} and A_{std} are the absorbances of the sample and standard at the excitation wavelength, and n_{unk} and n_{std} are the refractive indexes of the sample and standard solutions (pure solvents were assumed).

The emission lifetimes were measured by a quanta ray DCR-3 pulsed Nd:YAG laser system (pulse output 355 nm, 6 ns). The emission signals were collected by Hamamatsu R928 photomultiplier tube. Time-resolved difference absorption spectra were recorded after excitation of the sample in a degassed solution with a 8 ns laser pulse at $\lambda = 355$ nm. The monitoring beam provided by a 300 W continuous-wave xenon lamp was oriented perpendicular to the direction of the laser pulse. The absorption signal at each wavelength was collected with a SpectraPro-275 monochromator operating with 2 mm slits, with the signal recorded to a Tektronix TDS 350 oscilloscope. The optical difference spectrum was generated point-by-point by monitoring at individual wavelengths.

Luminescent Sensing Films. A series of solutions of [PtF_{28}TPP] with concentrations ranging from 1.67×10^{-5} to 1.67×10^{-4} mol dm^{-3} were prepared from their stock solutions (5×10^{-4} mol dm^{-3}) in tetrahydrofuran (THF) by transferring the required volume of complex solution and making up to a total of 1.5 mL with THF. Silicone rubber (0.2 g) was added to a solution, and the mixture was sonicated for 1 h. The resulting homogeneous paste (0.3 mL) was pipetted into a glass cell, which contained short glass tubing (11 mm in diameter × 10 mm in height) placed on the top of a glass slide. The cell was allowed to stand for 24 h for evaporation of solvent and completion of polymerization to give a film of about 0.2 mm in thickness. The complex concentration in each film was calculated by dividing the amount (in molar quantity) of the complex with the final volume of the sensing film.

For oxygen sensing experiments, the above glass cell with the platinum-porphyrin-containing film was mounted to a flow cell, and the oxygen concentration in the gas stream to the flow cell was regulated by controlling the relative flow rate of oxygen to nitrogen gas as previously described.[18] The film was aligned at 45° with respect to the excitation light source in the spectrofluorimeter. For alcohol sensing experiments, alcohol vapor of various concentrations in nitrogen gas stream were produced by diffusion tube method.[19] The experimental setup had been reported previously.[20]

X-ray Crystallography. Crystals of [PtF_{28}TPP] were obtained by slow diffusion of hexane into a dichloromethane solution. Crystal data and details of data collection and refinement are summarized in Table 1. Diffraction data of [PtF_{28}TPP] were collected on a MAR diffractometer with graphite monochromatized Mo Kα radiation ($\lambda = 0.71073$ Å). The images were interpreted and intensities integrated using the program *DENZO*.[21] The structure was solved by direct methods employing the SHELXS-97[22] program. The Pt atom was located according to direct methods. The positions of the other non-hydrogen atoms were found after successful refinement by full-matrix least-squares using the program SHELXL-97[23] on PC. One crystallographic asymmetric unit consists of one formula unit.

Table 1. Crystal Data

	[PtF_{28}TPP]
formula	$C_{44}F_{28}N_4Pt$
fw	1311.57
cryst size, mm^3	$0.50 \times 0.15 \times 0.03$
cryst syst	monoclinic
space group	$P2_1/c$
a, Å	15.402(3)
b, Å	10.341(2)
c, Å	28.085(6)
β, deg	92.07(3)
V, $Å^3$	4470.2(16)
Z	4
D_c, g cm^{-3}	1.949
μ, mm^{-1}	3.295
$2\theta_{max}$, deg	51.12
no. unique data	5657
no. obsd data ($I \geq 2\sigma(I)$)	3337
no. variables	694
R,[a] R_w[b]	0.050, 0.15
GOF	0.97
residual ρ, e$Å^{-3}$	+0.89, −1.21

[a] $R = \sum||F_o| - |F_c||/\sum|F_o|$. [b] $R_w = [\sum w(|F_o| - |F_c|)^2/\sum w|F_o|^2]^{1/2}$.

Results

Synthesis and Characterization. The H_2F_{28}TPP porphyrin was prepared[8] according to Lindsey's method,[24] by acid-catalyzed condensation of 3,4-difluoropyrrole[25] with pentafluorobenzaldehyde followed by oxidation with 2,3-dichloro-5,6-dicyano-1,4-benzoquinone (DDQ). A solution of H_2F_{28}TPP and [$PtCl_2(NCPh)_2$] in benzonitrile was heated at reflux to afford [PtF_{28}TPP] in ca. 80% yield as a dark red crystalline solid, which exhibits good solubility in common organic solvents including hexane, benzene, acetonitrile, and ethanol. The ^{19}F NMR spectrum of [PtF_{28}TPP] in $CDCl_3$ shows peaks in the −138.31 to −161.10 ppm range, comparable to the related values for H_2F_{28}TPP and [ZnF_{28}TPP].[8b,e] The fluorine resonances from all four *meso*-aryl rings appear to be equivalent in the ^{19}F NMR spectra, whereas the eight β-pyrrolic fluorine atoms appear as one singlet signal, thus suggesting that the structure of [PtF_{28}TPP] contains a high degree of symmetry.

(17) Demas, J. N.; Crosby, G. A. *J. Phys. Chem.* **1971**, *75*, 991−1024.
(18) Lee, W. W.-S.; Wong, K.-Y.; Li, X.-M.; Leung, Y.-B.; Chan, C.-S.; Chan, K. S. *J. Mater. Chem.* **1993**, *3*, 1031−1035.
(19) Altshuller, A. P.; Cohen, I. R. *Anal. Chem.* **1960**, *32*, 802−810.
(20) Lu, W.; Chan, M. C. W.; Zhu, N.; Che, C.-M.; He, Z.; Wong, K.-Y. *Chem. Eur. J.* **2003**, *9*, 6155−6166.
(21) Otwinowski, Z.; Minor, W. In *Processing of X-ray Diffraction Data Collected in Oscillation Mode*; Carter, C. W., Jr., Sweet, R. M., Eds.; Methods in Enzymology Vol. 276, Macromolecular Crystallography part A; Academic Press: New York, 1997; pp 307−326.
(22) *SHELXS97*: Sheldrick, G. M. *SHELX97, Programs for Crystal Structure Analysis*; University of Göttingen: Göttingen, Germany, 1997.
(23) *SHELXL97*: Sheldrick, G. M. *SHELX97, Programs for Crystal Structure Analysis*; University of Göttingen: Göttingen, Germany, 1997.
(24) Lindsey, J. S.; Schreiman, I. C.; Hsu, H. C.; Kearney, P. C.; Marguerettaz, A. M. *J. Org. Chem.* **1987**, *52*, 827−836.
(25) Leroy, J.; Wakselman, C. *Tetrahedron Lett.* **1994**, *35*, 8605−8608.

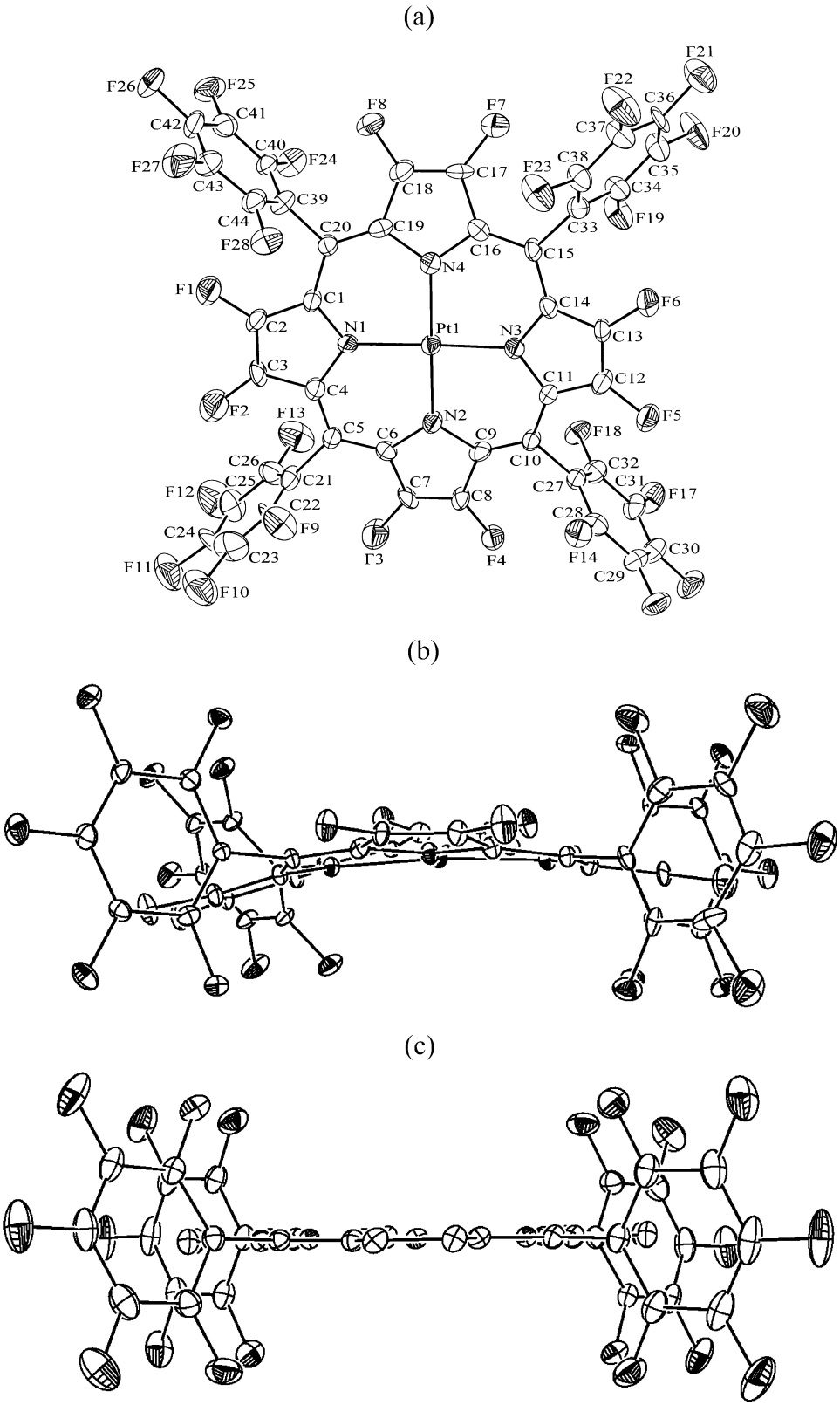

Figure 1. (a) Perspective view of [$PtF_{28}TPP$] (30% probability ellipsoids). Average bond lengths (Å) and angles (deg): Pt−N 2.008, N−C_α 1.398, C_α−C_β 1.423, C_β−C_β 1.337, C_α−C_{meso} 1.363; C_α−N−C_α 109.0, N−C_α−C_β 106.2, N−C_α−C_{meso} 126.6, C_α−C_β−C_β 109.3, C_α−C_{meso}−C_α 123.6, N(1)−Pt(1)−N(3) 174.8, N(3)−Pt(1)−N(4) 90.7. Views of (b) [$PtF_{28}TPP$] and (c) [$PtF_{20}TPP$][15] (30% thermal ellipsoids) along the porphyrin plane.

Perspective views of [$PtF_{28}TPP$] orthogonal to and along the porphyrin plane are shown in part a of Figure 1 and parts b and c in Figure 1, respectively. The platinum atom is nearly coplanar with the plane of the porphyrin ring with a slight displacement of 0.0119 Å. The mean platinum−nitrogen distance is 2.008 Å, which is comparable to the metal−nitrogen distances reported for [$MF_{20}TPP$] analogues (1.996, 2.036, and 2.018 Å for M = Cu,[9b] Zn,[9b] and Pt,[15] respec-

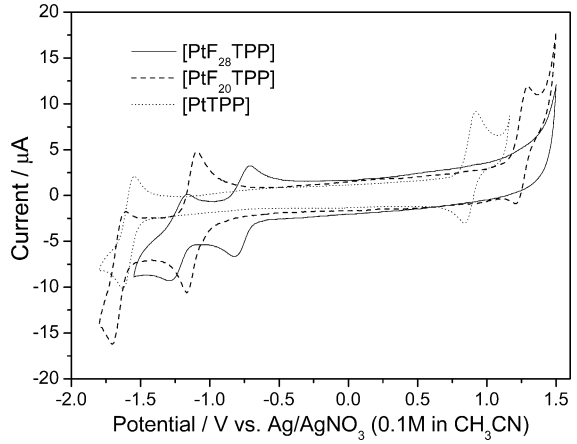

Figure 2. Cyclic voltammograms of [$PtF_{28}TPP$], [$PtF_{20}TPP$], and [PtTPP] (10^{-4} mol dm^{-3}) in CH_2Cl_2 containing 0.1 M $^nBu_4NPF_6$ as supporting electrolyte. Scan rate: 50 mV s^{-1}.

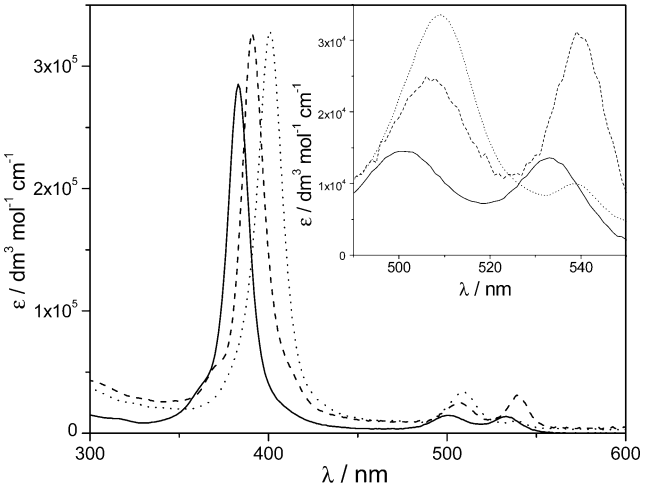

Figure 3. UV−vis absorption spectra of [$PtF_{28}TPP$] (—), [$PtF_{20}TPP$] (- - -), and [PtTPP] (···) in CH_2Cl_2 at 298 K. Inset: the low-energy Q(1,0) and Q(0,0) bands.

tively) and that of 2.059 Å in [$ZnF_{28}TPP$].[8b] The molecular structure reveals a slightly saddle-shaped conformation, whereby the fluorinated pyrrole rings, which are essentially planar, lie alternately above and below the porphyrin mean plane. The largest average deviations of 0.49 Å from the porphyrin mean plane occur at the β-pyrrolic carbon atoms (C_β). This is in stark contrast to the virtually planar porphyrin core reported for [$PtF_{20}TPP$][15] (Figure 1c), in which case the platinum atom is located at the crystallographic inversion center of the molecule. The *meso*-pentafluorophenyl rings in [$PtF_{28}TPP$] are essentially orthogonal to the porphyrin core, like those in [$PtF_{20}TPP$].[15] In the crystal lattice of [PtF_{28}-TPP], intermolecular nonbonded C···F contacts between *meso*-aryl fluorine atoms and α- or β-pyrrolic carbon (average 3.09 Å, shortest 3.02 Å) and between adjacent *meso*-pentafluorophenyl rings (average 3.1 Å) are observed above and below the porphyrin plane.

The electrochemical properties of [$PtF_{28}TPP$], [$PtF_{20}TPP$], and [PtTPP] in CH_2Cl_2 solution have been investigated by cyclic voltammetry at 298 K using 0.1 M $^nBu_4NPF_6$ as supporting electrolyte, and are depicted in Figure 2. For [$PtF_{28}TPP$], there is no oxidation peak even up to a potential of 1.5 V, whereas for [$PtF_{20}TPP$] and [PtTPP], there is a reversible oxidation wave at $E_{1/2}$ = 1.33 and 0.97 V, respectively. The two porphyrinato ring-centered reduction waves of [$PtF_{28}TPP$] (−0.75 and −1.18 V) occur at potentials anodically shifted from those of [$PtF_{20}TPP$] (−1.06 and −1.55 V). For [PtTPP], the first reduction wave occurs at an $E_{1/2}$ value of −1.51 V.

Absorption Spectroscopy. The UV−vis absorption data of [$PtF_{28}TPP$], [$PtF_{20}TPP$], and [PtTPP] in various solvents are listed in Table 2, and their spectra in dichloromethane are shown in Figure 3. The [$PtF_{28}TPP$] complex exhibits a near-UV Soret band (B) at 383 nm and two Q(1,0) and Q(0,0) bands at 501 and 533 nm, respectively, in dichloromethane. The relative extinction coefficients for the Q(0,0) and Q(1,0) transitions of the three complexes are listed in Table 2 and portrayed in Figure 3 (inset). The ratio of the ϵ values for [$PtF_{28}TPP$] (0.94) is slightly smaller than that of [$PtF_{20}TPP$] (1.27), while both are significantly larger than that of [PtTPP] (0.30) in CH_2Cl_2 solution. This is consistent with the Gouterman four-orbital parameters[26] and Shelnutt and Oritz's[27] quantitative method of analysis, which rationalize the substituent effect upon the $\pi-\pi^*$ transitions of metalloporphyrins. The B(0,0)−Q(0,0) spectral splitting decreases in the order [$PtF_{28}TPP$] > [$PtF_{20}TPP$] > [PtTPP].

The solvent effect on the absorption spectrum of [PtF_{28}-TPP] has been examined (Table 2). When the solvent is changed from dichloromethane to pyridine, the Soret band absorption red-shifts by 270 cm^{-1}, but the shift in the Q-band energies is negligible. The ϵ values for the Soret absorption recorded in various solvents lie between 2.5 × 10^5 and 3.1 × 10^5 dm^3 mol^{-1} cm^{-1}, whereas the Q-band absorption bands

Table 2. Absorption Data of [$PtF_{28}TPP$], [$PtF_{20}TPP$], and [PtTPP] in Various Solvents

complex	solvent	λ_{max}/nm (ϵ/dm^3 mol^{-1} cm^{-1})		Q(0,0)/Q(1,0) ϵ ratio	B(0,0)−Q(0,0) splitting ν/cm^{-1}
		Soret (B band)	Q(1,0) and Q(0,0) bands		
[$PtF_{28}TPP$]	hexane	382 (312 000)	500 (16 400), 532 (14 400)	0.88	7381
	CCl_4	384 (295 000)	501 (18 900), 532 (17 600)	0.93	7245
	CH_2Cl_2	383 (285 000)	501 (14 500), 533 (13 600)	0.94	7348
	benzene	386 (260 000)	502 (14 300), 533 (12 900)	0.90	7145
	THF	383 (292 000)	502 (24 200), 535 (22 300)	0.92	7418
	acetonitrile	381 (286 000)	501 (14 000), 533 (12 700)	0.91	7485
	MeOH	381 (289 000)	500 (14 200), 532 (12 800)	0.90	7450
	EtOH	382 (256 000)	500 (12 300), 534 (10 800)	0.88	7451
	pyridine	387 (250 000)	502 (14 600), 535 (13 100)	0.90	7148
[$PtF_{20}TPP$]	CH_2Cl_2	390 (323 000)	504 (23 200), 538 (29 400)	1.27	7054
	Benzene	394 (220 000)	509 (13 400), 540 (18 100)	1.35	6862
[PtTPP]	CH_2Cl_2	401 (329 000)	509 (33 600), 539 (9960)	0.30	6385

Table 3. Solution Emission Data for [$PtF_{28}TPP$], [$PtF_{20}TPP$], and [PtTPP] in Various Solvents (Concentration 1.5×10^{-6} mol dm^{-3})

complex	solvent	λ_{em}/nm	Φ	τ^b/μs	E_K
[$PtF_{28}TPP$]	hexane	651, 715 (sh)	0.076	9.3	48.9
	CCl_4	648, 705 (sh)	0.047	6.2	49.9
	CH_2Cl_2	650, 712 (sh)	0.043	5.8	53.9
	benzene	651, 704 (sh)	0.033	5.3	53.4
	THF	650, 715 (sh)	0.028	4.4	55.4
	acetonitrile	651, 718 (sh)	0.012	1.3	59.0
	MeOH	650, 715 (sh)[a]	0.0003	<0.1[c]	56.3
	EtOH	652, 717 (sh)[a]	0.0002	<0.1[c]	55.3
	pyridine	nonemissive			57.0
[$PtF_{20}TPP$]	hexane	647, 705 (sh)	0.081	52	48.9
	CH_2Cl_2	647, 710 (sh)	0.088	60	53.9
	benzene	649, 710 (sh)	0.070	26	53.4
	acetonitrile	647, 705 (sh)	0.084	55	59.0
	MeOH	647, 705 (sh)	0.045	26	56.3
[PtTPP]	CH_2Cl_2	665, 730 (sh)	0.046	50	53.9

[a] Weakly emissive. [b] Measured at λ_{max}. [c] Estimated lifetime due to weak emission.

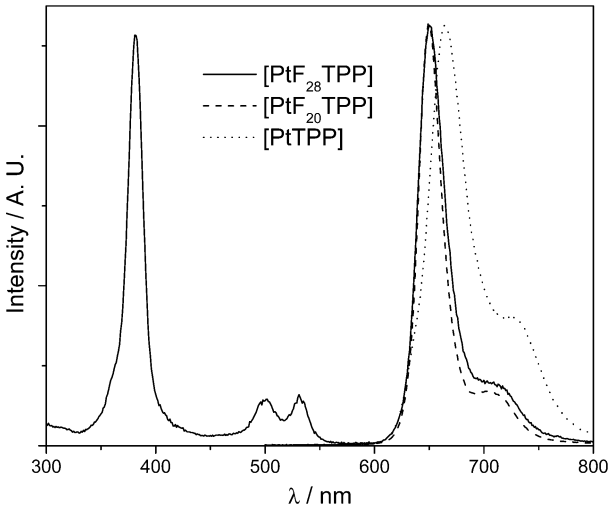

Figure 4. Excitation and emission spectra of [$PtF_{28}TPP$] in dichloromethane at 298 K (concentration 1.5×10^{-6} mol dm^{-3}, λ_{ex} 390 nm; emission spectra of [$PtF_{20}TPP$] and [PtTPP] also shown).

exhibit ϵ values ranging from 1.0×10^4 to 2.4×10^4 dm^3 mol^{-1} cm^{-1}. The relative Q(0,0)/Q(1,0) intensity ratios vary in the range 0.88−0.94, and the B(0,0)−Q(0,0) spectral splitting occurs between 7145 and 7485 cm^{-1}.

Luminescence Spectroscopy. The complexes [$PtF_{28}TPP$], [$PtF_{20}TPP$], and [PtTPP] show intense phosphorescence in solutions at room temperature; their photophysical data are listed in Table 3. Figure 4 shows the excitation and emission spectra of [$PtF_{28}TPP$] in CH_2Cl_2 at 298 K. The emission profile of [$PtF_{28}TPP$] is nearly identical to that of [PtF_{20}-TPP]. With reference to previous work,[15] the narrow peak at 650 nm (680 cm^{-1} full width at half-maximum intensity) and weak band at 712 nm are attributed to the excited triplet states of the Q-bands. When monitoring the emission wavelength at 650 nm, the excitation spectrum exhibits an intense Soret band at 382 nm and the Q(1,0) and Q(0,0) bands at 500 and 532 nm, respectively, which correspond to the ground-state absorption spectrum in Figure 3. A self-quenching experiment on the emission of [$PtF_{28}TPP$] was performed in the concentration range 1.98×10^{-6} to 3.96×10^{-5} mol dm^{-3} in CH_2Cl_2 at 298 K, but no detectable quenching effect was found. The 77 K glassy emission of [$PtF_{28}TPP$] in MeOH/EtOH (1:4) shows blue-shifted emission with an intense peak maximum at λ_{max} 639 nm ($\tau = 56$ μs) and two weaker bands at 691 and 708 nm. In deoxygenated hexane solution, the emission lifetime and quantum yield of [$PtF_{28}TPP$] are 9.3 μs and 0.076, which decrease to 0.4 μs and 0.004, respectively, under aerated conditions.

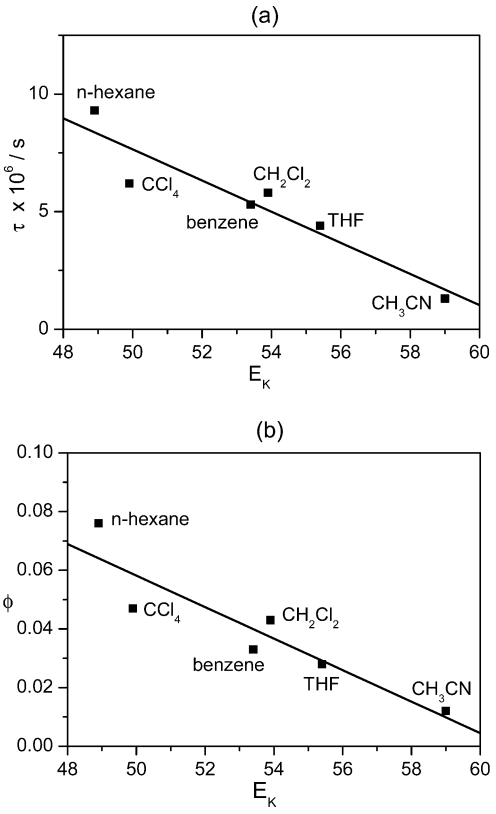

Figure 5. Plot of emission lifetime (a) and quantum yield (b) for [PtF_{28}-TPP] against the E_K scale.

The effect of solvent upon the emission of [$PtF_{28}TPP$] and [$PtF_{20}TPP$] (complex concentration = 1.5×10^{-6} mol dm^{-3}) has been examined (Table 3; see Supporting Information for spectra). Although the emission maxima for both complexes are insensitive to solvent polarity, the emission quantum yield (Φ) for [$PtF_{28}TPP$] decreases from 0.076 in hexane to <0.001 in methanol and ethanol, while that for [$PtF_{20}TPP$] shows only minor solvent dependence (from 0.088 in CH_2Cl_2 to 0.045 in methanol). In addition, the emission lifetime of [$PtF_{28}TPP$] at 298 K exhibits a pronounced solvent dependence and varies from 9.3 μs in hexane to <0.1 μs in methanol, whereas the emission lifetime of [$PtF_{20}TPP$] shows only a slight variation with solvent polarity (range 26−60 μs). We note that a linear correlation is evident between the polarity of solvent, defined by the E_K value (where solvent polarities are classified with respect to the hypsochromic shift of the longest wavelength absorption of the [$Mo(CO)_4$-{$(C_5H_4N)HC{=}NCH_2C_6H_5$}] complex[28]), and the lifetime or quantum yield of [$PtF_{28}TPP$], as depicted in Figure 5a,b.

Excited-State Properties. The triplet excited-state absorption spectrum of [$PtF_{28}TPP$] (1.5×10^{-6} mol dm^{-3}) in

(26) Gouterman, M. In *The Porphyrins*; Dolphin, D., Ed.; Academic: New York, 1978; Vol. III, pp 1−165.
(27) Shelnutt, J. A.; Ortiz, V. *J. Phys. Chem.* **1985**, *89*, 4733−4739.

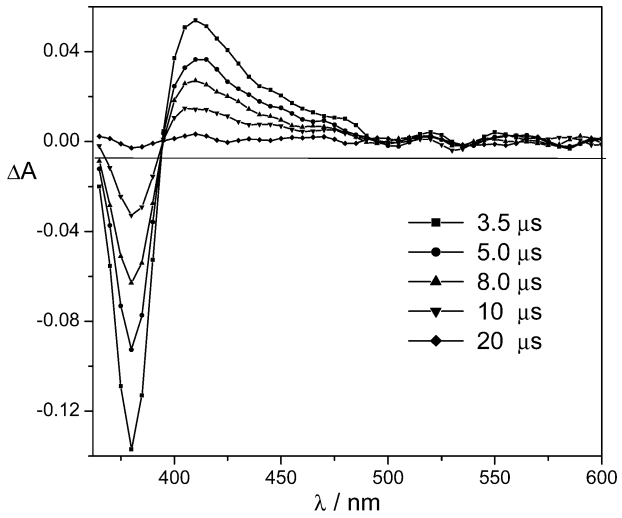

Figure 6. Time-resolved differential absorption spectra of [PtF_{28}TPP] (1.5×10^{-6} mol dm^{-3}) monitored at 3.5−20 μs after pulsed excitation at $\lambda =$ 355 nm in degassed hexane.

deoxygenated hexane was recorded 3.5−20 μs after laser flash photolysis of the solution at 355 nm. As depicted in Figure 6, the difference absorption spectrum shows an absorption maximum at 410 nm, which decays with a half-life of 8.9 μs. The solvent effect on the triplet excited-state absorption spectrum has been examined: the peak maximum remains at ~410 nm, while the decay half-life was found to be 5.1 and 1.5 μs in CH_2Cl_2 and CH_3CN solution, respectively (see Supporting Information). These decay lifetimes closely match the corresponding emission lifetimes (Table 3; 9.3 μs in hexane, 5.8 μs in CH_2Cl_2, and 1.3 μs in CH_3CN). We attribute the 410 nm band to the intraligand $^3(\pi,\pi^*)$ excited state of [PtF_{28}TPP].[29] In aerated dichloromethane solution (2.5×10^{-6} mol dm^{-3}), the differential absorption spectrum remains the same except that the 410 nm band decays with a shorter half-life (1.1 μs) due to quenching of the [PtF_{28}TPP] emission by oxygen (see later).

The excited-state potential of [PtF_{28}TPP] can be estimated using the spectroscopic and electrochemical data. The 0−0 transition energy E_{0-0}, which can be approximated from the overlap of the emission and excitation spectra, occurs at ca. 2.24 eV, and $E_{1/2}$ for [$PtF_{28}TPP + e^- \rightarrow (PtF_{28}TPP)^-$] is −0.75 V versus Ag/$AgNO_3$. Thus, the triplet excited state of [PtF_{28}TPP] is a powerful oxidant with the $E_{1/2}$ for [$(PtF_{28}TPP)^* + e^- \rightarrow (PtF_{28}TPP)^-$] estimated to be ca. 1.49 V versus Ag/$AgNO_3$. The powerful oxidizing nature of [PtF_{28}TPP]* has been demonstrated by the quenching of the emission by 1,2,4-trimethoxybenzene, and the quenching mechanism was found to occur via an electron-transfer pathway. The differential absorption spectrum of a degassed acetonitrile solution of [PtF_{28}TPP] (1.5×10^{-6} mol dm^{-3}) and 1,2,4-trimethoxybenzene (5 mol dm^{-3}), recorded after excitation, shows a prominent absorption band at 450 nm, which can be attributed to the formation of the 1,2,4-trimethoxybenzene radical cation.[30] Using Stern−Volmer analysis, the quenching rate constant of [PtF_{28}TPP] by 1,2,4-trimethoxybenzene was determined to be 2.61×10^9 dm^3 mol^{-1} s^{-1}.

Table 4. Rate Constants for the Quenching of [PtF_{28}TPP] by Various Substrates in Dichloromethane unless Otherwise Stated

quencher	k_q/dm^3 mol^{-1} s^{-1}
methanol	1.34×10^6
N,*N*-dimethylformamide	7.56×10^6
cyclohexene	3.16×10^7
deuterated cyclohexene (C_6D_{10})	3.19×10^7
pyridine	2.33×10^8
triphenylphosphine	1.30×10^9
tetrahydrothiophene	2.39×10^9
1,2,4-trimethoxybenzene	2.61×10^9
butylamine[a]	5.64×10^8
catechol[a]	3.32×10^9

[a] Measured in acetonitrile.

The emission of [PtF_{28}TPP] in solution is sensitive to the presence of substrates. Quenching experiments were performed in dichloromethane or acetonitrile solutions upon addition of different substrates at 298 K and linear Stern−Volmer plots of $1/\tau$ of [PtF_{28}TPP] against substrate concentration have been obtained (quenching rate constants, k_q/dm^3 mol^{-1} s^{-1} determined in the Supporting Information). The results of quenching rate constants (k_q) are listed in Table 4. The k_q value for deuterated cyclohexene (C_6D_{10}) in dichloromethane is 3.19×10^7 dm^3 mol^{-1} s^{-1}, which is nearly identical to that of 3.16×10^7 dm^3 mol^{-1} s^{-1} for cyclohexene (C_6H_{10}), suggesting no C−H isotope effect for the quenching process. The k_q values for the emission of [PtF_{28}TPP] and [PtF_{20}TPP] (~2×10^{-6} mol dm^{-3}) by pyridine in dichloromethane solution were found to be 2.33×10^8 and 2.17×10^7 dm^3 mol^{-1} s^{-1}, respectively.

Photostability and Luminescent Quenching Studies. The photostabilities of [PtF_{28}TPP], [PtF_{20}TPP], and [PtTPP] in thin silicone film were examined by broad-band irradiation with a high-power mercury arc lamp (500 W) for 14 h under aerobic conditions (Figure 7). Both [PtF_{28}TPP] and [PtF_{20}TPP] exhibited high photostability with 97% and 90%, respectively, of their emission intensities retained after irradiation. In contrast, only 12% of the emission intensity remained for the nonfluorinated congener [PtTPP] under identical irradiation conditions.

The sensitivity of the emission of [PtF_{28}TPP] encapsulated in silicone film toward dioxygen was examined by recording the relative emission intensity at λ_{max} 645 nm before (I_0) and after (I) purging oxygen (% in vol/vol) into the system (Figure 8). First, a series of films containing different concentrations of [PtF_{28}TPP] were used, and the optimal complex concentration of [PtF_{28}TPP] which gave the highest sensitivity (highest I_0/I ratio) was found to be 0.24 mM. A linear correlation between the relative emission intensity (I_0/I) of [PtF_{28}TPP] recorded at 645 nm and the concentration of oxygen (% vol/vol) purged into the system is observed (Figure 8). Although the Stern−Volmer plots for most

(28) (a) Walther, D. *J. Prakt. Chem.* **1974**, *316*, 604−614. (b) Kamlet, M. J.; Abboud, J. L. M.; Taft, R. W. In *Progress in Physical Organic Chemistry*; Taft, R. W., Ed.; Wiley: New York, 1981; Vol. 13, pp 485−630. (c) Reichardt, C. *Solvents and Solvent Effects in Organic Chemistry*; Wiley-VCH: Weinheim, 2003; Chapter 7, pp 389−469.
(29) Rodriguez, J.; Kirmaier, C.; Holten, D. *J. Am. Chem. Soc.* **1989**, *111*, 6500−6506.
(30) O'Neill, P.; Steenken, S.; Schulte-Frohlinde, D. *J. Phys. Chem.* **1975**, *79*, 2773−2779.

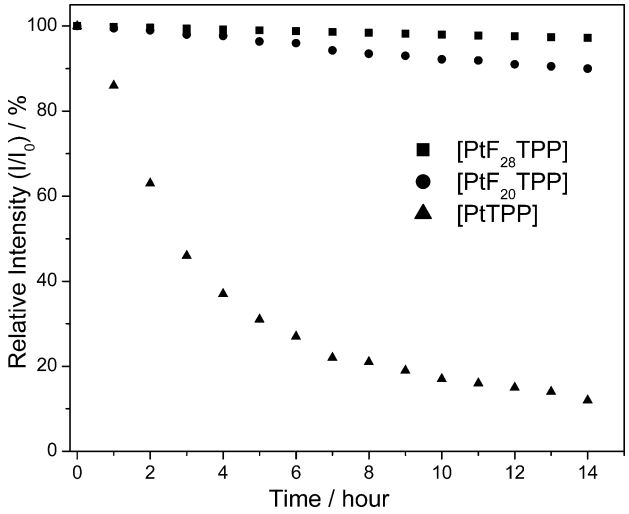

Figure 7. Photostability studies on silicone films of [PtF_{28}TPP], [PtF_{20}TPP], and [PtTPP]: plot of relative emission intensity versus time of irradiation.

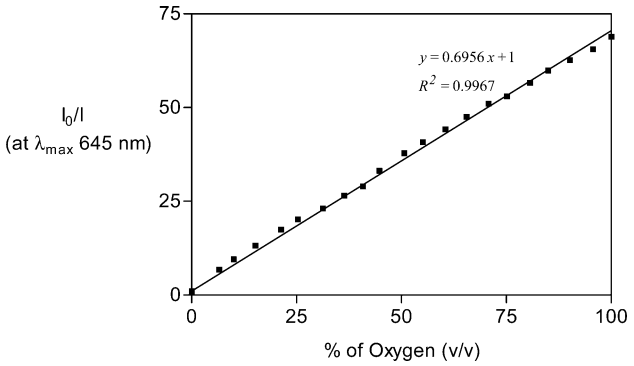

Figure 8. Oxygen sensitivity of silicone-encapsulated [PtF_{28}TPP]: plot of relative emission intensity (I_0/I) at λ_{max} 645 nm versus exposure of oxygen (% in vol/vol).

oxygen sensors based on polymer-embedded luminophores are nonlinear,[31] linear calibration plots (I_0/I versus concentration) have previously been reported for platinum porphyrins encapsulated in silicone rubber[32] and PVC matrix.[33] The linear Stern−Volmer plot for [PtF_{28}TPP] can be attributed to a better mixing of the hydrophobic platinum porphyrin with silicone rubber, resulting in a more homogeneous matrix. The I_0/I_{100} ratio for [PtF_{28}TPP] reaches 69 in the presence of 100% oxygen, which is comparable to those values reported for other platinum porphyrins.[18]

Similar studies on the sensitivity of the emission of silicone-encapsulated [PtF_{28}TPP] film toward methanol or ethanol were also undertaken. The [PtF_{28}TPP] complex exhibited a decrease in emission intensity recorded at 645 nm upon exposure to these two alcohols. As depicted in Figure 9, the plots of relative emission intensities (I_0/I) against the concentration of alcohol vapor (in ppm) are linear up to alcohol concentrations of 200 and 140 ppm for methanol and ethanol, respectively. The detection limit of

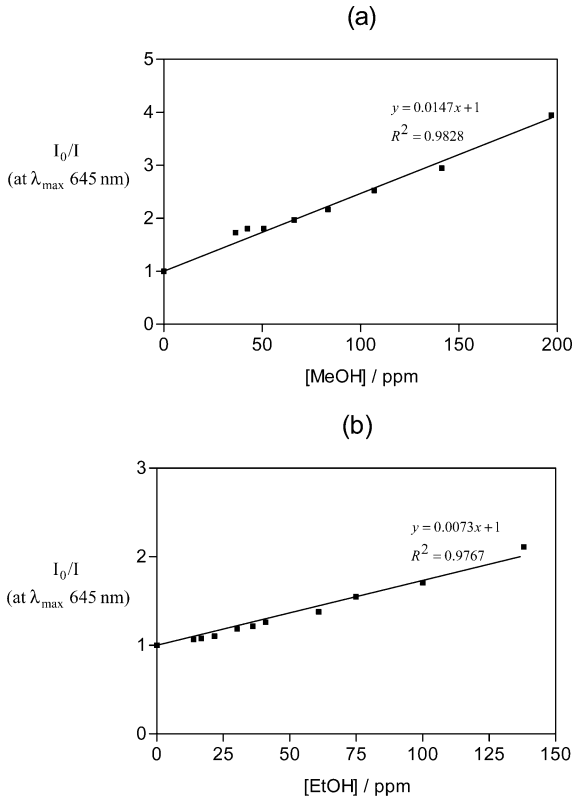

Figure 9. Alcohol sensitivity of silicone-encapsulated [PtF_{28}TPP]: plot of relative emission intensity (I_0/I) at λ_{max} 645 nm versus exposure to (a) methanol and (b) ethanol (in ppm).

the [PtF_{28}TPP] film was found to be 36 ppm for methanol and 13 ppm for ethanol.

Discussion

Structural, Photophysical, and Electrochemical Features. In the molecular structure of [PtF_{28}TPP], the *meso*-pentafluorophenyl substituents are orthogonal to the porphyrin core to relieve steric encumbrance between the C_6F_5 rings and β-pyrrolic fluorine atoms at the porphyrin periphery. The electronic effect of fluorine-substituted phenyl rings can be inductively transmitted to the porphyrin ring. The saddle-shaped distortion of the porphyrin core in [PtF_{28}TPP] (Figure 1b), in contrast to the planar geometry of [PtF_{20}TPP] (Figure 1c), implies the presence of additional steric congestion between the β-pyrrolic fluorine atoms and the pentafluorophenyl moieties, while the strong σ electron-withdrawing effect of the eight β-fluorine substituents may also play a part. This structural distortion is similarly observed in the [β-octabromo-*meso*-tetrakis(pentafluorophenyl)porphyrinato]zinc(II) complex,[34] but only slight ruffling is present in the structure of [ZnF_{28}TPP].[8b]

The Soret absorption at 26110 cm^{-1} (383 nm) of [PtF_{28}TPP] in dichloromethane occurs at a higher energy compared to that of 25 641 cm^{-1} (390 nm) for [PtF_{20}TPP] and 24 938 cm^{-1} (401 nm) for [PtTPP] (Figure 3). Fluorination at β-pyrrolic positions of the porphyrin macrocycle apparently induces a significant electron-withdrawing effect, which

(31) Demas, J. N.; DeGraff, B. A.; Coleman, P. B. *Anal. Chem.* **1999**, *71*, 793A−800A.
(32) Kavandi, J.; Callis, J.; Gouterman, M.; Khalil, G.; Wright, D.; Green, E.; Burns, D.; McLachlan, B. *Rev. Sci. Instrum.* **1990**, *61*, 3340−3347.
(33) Hartmann, P.; Trettnak, W. *Anal. Chem.* **1996**, *68*, 2615−2620.
(34) Marsh, R. E.; Schaefer, W. P.; Hodge, J. A.; Hughes, M. E.; Gray, H. B. *Acta Crystallogr.* **1993**, *C49*, 1339−1342.

propagates through the macrocyclic ring and substantially modulates the a_{2u}/a_{1u} orbital energies, resulting in a blue-shifted Soret absorption. The B(0,0)−Q(0,0) spectral splitting decreases in the order [PtF_{28}TPP] > [PtF_{20}TPP] > [PtTPP], which also suggests that the *meso*-C_6F_5 rings and β-fluorine substituents are effective in removing electron density from the porphyrinato nitrogen atoms, thereby widening the HOMO−LUMO gap in the chromophores. The hypsochromic shift in the absorption spectrum of [PtF_{28}TPP] signifies that the inductive effect of the eight β-fluorine atoms outweighs the expected bathochromic shift arising from distortion of the porphyrin core from planarity.

The one-electron redox potentials of porphyrins often reflect the energy levels of their HOMOs and LUMOs.[35] Compared to [PtF_{20}TPP], the cyclic voltammogram of [PtF_{28}TPP] shows an anodic shift (Figure 2) in potentials for both the porphyrinato oxidation and reduction, implying that β-pyrrolic fluorination removes electron density from the porphyrin ring. Hence, the [PtF_{28}TPP] complex is easily reduced and resistant to oxidation relative to its [PtF_{20}TPP] and [PtTPP] analogues. The estimated excited-state potential (ca. 1.49 V vs $Ag/AgNO_3$) also signifies that [PtF_{28}TPP] is a powerful one-electron photo-oxidant.

The emission spectrum of [PtF_{28}TPP] is similar to that of [PtF_{20}TPP] (Figure 4) with the peak maximum at ~650 nm attributed to the excited Q(0,0) triplet state. The emission lifetime and quantum yield (τ ranges from <0.1 to 9.3 μs and Φ from <0.001 to 0.076) of [PtF_{28}TPP] decrease notably from those observed for [PtF_{20}TPP] (τ = 26−60 μs; Φ = 0.045−0.088) in various solvents. Interestingly, both the emission lifetime and quantum yield of [PtF_{28}TPP] decrease in a linear fashion with an increase in solvent polarity expressed as E_K values (Figure 5), while [PtF_{20}TPP] shows no such correlation. A comparison between the quenching rate constants by pyridine on the emission of [PtF_{28}TPP] and [PtF_{20}TPP] (2.33×10^8 and 2.17×10^7 dm^3 mol^{-1} s^{-1}, respectively) shows that the former is more prone to quenching by nitrogen donors. This suggests the structural and electronic differences of [PtF_{28}TPP] from [PtF_{20}TPP] (as discussed above) promote its solvent-induced nonradiative decay rates. First, the incorporation of fluorine atoms at both *meso*-phenyl and β-pyrrolic carbons in [PtF_{28}TPP] causes deviation of the porphyrin core from planarity; this structural change may increase the dipole moment in the excited state, resulting in a more pronounced effect with change of solvent.[36] Second, the fluorine substituents at the β-pyrrolic positions of [PtF_{28}TPP] can confer electron-withdrawing effects upon the porphyrinato ring, which in turn promote porphyrin−solvent/substrate interactions in the excited state. Also, specific solvation might induce variations in the degree of ruffling for the structure of [PtF_{28}TPP] in the solvent.

Emission Quenching Studies of [PtF_{28}TPP]. The noticeably higher sensitivity of the emission of [PtF_{28}TPP] toward solvent polarity is intriguing in the development of luminescent sensing and signaling probes.[37] Indeed, quenching experiments performed in this work revealed relatively high quenching rate constants for soft and/or electron-rich donors such as triphenylphosphine (1.30×10^9 dm^3 mol^{-1} s^{-1}), tetrahydrothiophene (2.39×10^9 dm^3 mol^{-1} s^{-1}), catechol (3.32×10^9 dm^3 mol^{-1} s^{-1}), and butylamine (5.64×10^8 dm^3 mol^{-1} s^{-1}), which approach the diffusion-controlled limit.

Superior photostability has been observed for [PtF_{28}TPP], and 97% of emission intensity was retained after 14 h of broad-band irradiation with a high power mercury arc lamp (Figure 7). The β-fluorination of the porphyrin core evidently confers improved photostability. Studies on the sensitivity of the emission of [PtF_{28}TPP]-incorporated silicone film toward dioxygen, methanol, or ethanol revealed that, over a wide concentration range of these substrates, linear calibration curves of the emission intensity ratio (I_0/I) versus concentration can be obtained (Figures 8 and 9). The I_0/I_{100} ratio of [PtF_{28}TPP] film recorded at 645 nm reached a maximum value of 69 in the presence of pure oxygen (Figure 8), suggesting the potential use of [PtF_{28}TPP] as a robust luminescent sensory material for detection of dioxygen.

Conclusion

Spectroscopic and electrochemical studies on the perfluorinated [PtF_{28}TPP] complex indicate that the incorporation of fluorine atoms at the β-positions of the porphyrin ring has a modest effect upon the electronic properties, but the oxidation potentials are markedly increased for both the ground and excited states, which enhances the resistance toward oxidative degradation. The triplet excited state of [PtF_{28}TPP] is a powerful oxidant. The β-fluoro substituents in [PtF_{28}TPP] render blue-shifts for the Soret and Q-bands in the absorption spectrum. Good photostability and remarkable solvent dependence of emission lifetime and quantum yield for [PtF_{28}TPP] have been observed. Finally, the emission quenching of [PtF_{28}TPP] has been demonstrated by diminution of the emission intensity upon exposure to oxygen and alcohol. Employment of platinum-porphyrin derivatives immobilized in polymer or Nafion as oxygen sensors was documented previously.[38]

Acknowledgment. We are grateful for financial support from The University of Hong Kong, Research Grants Council of the Hong Kong SAR, China [HKU 7039/03P], and Area of Excellence Scheme (AoE/P-10/01) of the University Grants Committee of the Hong Kong SAR, China.

Supporting Information Available: Crystal data for [PtF_{28}TPP] (CIF), emission spectra of [PtF_{28}TPP] and [PtF_{20}TPP] in various solvents, Stern−Volmer plots of [PtF_{28}TPP] using different electron-donating quenchers, and time-resolved differential absorption spectra of [PtF_{28}TPP]. This material is available free of charge via the Internet at http://pubs.acs.org.

IC049902H

(35) Barkigia, K. M.; Renner, M. W.; Furenlid, L. R.; Medforth, C. J.; Smith, K. M.; Fajer, J. *J. Am. Chem. Soc.* **1993**, *115*, 3627−3635.
(36) Retsek, J. L.; Medforth, C. J.; Nurco, D. J.; Gentemann, S.; Chirvony, V. S.; Smith, K. M.; Holten, D. *J. Phys. Chem. B* **2001**, *105*, 6396−6411.
(37) Nair, R. B.; Cullum, B. M.; Murphy, C. J. *Inorg. Chem.* **1997**, *36*, 962−965.
(38) (a) Vasil'ev, V. V.; Borisov, S. M. *Sens. Actuators, B* **2002**, *82*, 272−276. (b) Gillanders, R. N.; Tedford, M. C.; Crilly, P. J.; Bailey, R. T. *Anal. Chim. Acta* **2004**, *502*, 1−6.